Improvement Performances of the SMO Observer for PMSM Sensorless Control Based on DTC Strategy Using Simulated Annealing and Reinforcement Learning TD3 Agent

Marcel Nicola
Department of Automatic Control and Electronics
University of Craiova
Craiova, Romania
marcel.nicola@edu.ucv.ro

Claudiu-Ionel Nicola
Department of Automatic Control and Electronics
University of Craiova
Craiova, Romania
claudiu.nicola@edu.ucv.ro

Cătălin Constantinescu
Department of Automatic Control and Electronics
University of Craiova
Craiova, Romania
catalin.constantinescu@edu.ucv.ro

Răzvan Prejbeanu
Department of Automatic Control and Electronics
University of Craiova
Craiova, Romania
razvan.prejbeanu@edu.ucv.ro

***Abstract*—From the elements that contribute to increasing the reliability of the control system of a Permanent Magnet Synchronous Motor (PMSM), could be enumerated the replacement of the speed transducers with software-implemented speed observers. On this basis, this paper focuses on the sensorless regulation of a PMSM using a Direct Torque Control (DTC) type strategy, in which a speed observer is used in combination with a Reinforcement Learning-Twin Delayed Deep Deterministic Policy Gradient (RL-TD3) type agent to increase the accuracy of the PMSM rotor speed estimate. Simulated Annealing (SA) is also used to achieve superior performance of the velocity observer for optimal tuning of the PI-type velocity controller parameters. The latter can, after the training phase, provide correction signals to the speed observer so that the estimated speed is as close as possible to the estimated speed. The control structures, control algorithms, and operating equations of the PMSM, the control strategy of the DTC type, and the speed observer are presented in this paper. Numerical simulations carried out in the Matlab/Simulink programming environment validate the superiority of the PMSM rotor speed estimation performance in the case of the use of an RL-TD3-type agent in combination with a speed observer, compared to the case of the use of the speed observer alone.**

Keywords—PMSM, DTC, Simulated Annealing, SMO, Reinforcement Learning.

I. INTRODUCTION

The use of speed observers for PMSM rotor speed estimation eliminates the need for direct speed measurement using dedicated transducers, thereby increasing the overall reliability of the PMSM measurement and control system by eliminating mechanical elements whose wear and reliability can degrade overall system performance over time [1-6]. As far as the PMSM control strategies are concerned, there are two that are worth mentioning: Field Oriented Control (FOC) [7-10] and DTC [11-14]. With regard to the FOC strategy, it can be said that it offers superior performance to the DTC strategy because the controllers used in both the inner and outer loops have the minimum complexity guaranteed by the use of PI-type controllers. In the case of the DTC control strategy, it is considered advantageous to use a simple ON-OFF hysteresis control structures on the inner control loops, but with a slight degradation in the global PMSM performance control system.

As far as velocity observers are concerned, we mention their implementations using the Sliding Mode Observer (SMO) algorithm [15], Luenberger [16], Model Reference Adaptive System (MRAS) [17], and Kalman [18] in the case of the stochastic approach. Among these observers, those using the SMO algorithm show very good and robust behavior.

This paper is based on [6] and presents some improvements on obtaining superior velocity observer results by tuning velocity controller parameters using an SA-type algorithm. Thus, in this paper are presented a speed observer based on the initial estimation of the stator flux using an SMO-type observer, and the superior performance for the PMSM rotor speed estimation is obtained by using an RL-TD3 agent algorithm [19-22].

The rest of the paper is organized as follows: Section II shows the proposed sensorless control system for PMSM based on the DTC-type control strategy, and Section III presents the improvement of the SMO-type observer performance employing the RL-TD3-type agent. The Matlab/Simulink implementation of the proposed PMSM sensorless control system and the numerical simulation are shown in Section IV. The last section presents some conclusions and ideas for future work.

II. PROPOSED PMSM SENSORLESS CONTROL SYSTEM BASED ON DTC STRATEGY

In general terms, the PMSM operating equations in the *d-q* rotating reference frame are given by (1)-(4) [10-13].

$$\begin{bmatrix} \lambda_d \\ \lambda_q \end{bmatrix} = \begin{bmatrix} L_d & 0 \\ 0 & L_q \end{bmatrix} \begin{bmatrix} i_d \\ i_q \end{bmatrix} + \begin{bmatrix} \lambda_0 \\ 0 \end{bmatrix} \tag{1}$$

Cite as: M. Nicola, C.-I. Nicola, C. Constantinescu, and R. Prejbeanu, "Improvement Performances of the SMO Observer for PMSM Sensorless Control Based on DTC Strategy Using Simulated Annealing and Reinforcement Learning TD3 Agent", *Syst. Theor. Control Comput. J.*, vol. 3, no. 2, pp. 36–43, Dec. 2023.
DOI: 10.52846/stccj.2023.3.2.57

$$\begin{bmatrix} u_d \\ u_q \end{bmatrix} = R_s \begin{bmatrix} i_d \\ i_q \end{bmatrix} + \begin{bmatrix} L_d & 0 \\ 0 & L_q \end{bmatrix} \frac{d}{dt} \begin{bmatrix} i_d \\ i_q \end{bmatrix} + + n_p \omega \begin{bmatrix} 0 & -L_d \\ L_d & 0 \end{bmatrix} \begin{bmatrix} i_d \\ i_q \end{bmatrix} + n_p \omega \begin{bmatrix} 0 \\ \lambda_0 \end{bmatrix} \quad (2)$$

$$T_e = \frac{3}{2} n_p \left((L_d - L_q) i_d i_q + \lambda_0 I_q \right) \quad (3)$$

$$J\dot{\omega} = T_e - T_L - B\omega \quad (4)$$

where: indices *d* and *q* for circuit quantities *L* and *R*, but also for currents, voltages, and fluxes *i*, *u*, and λ are the projections on the *d*-axis and *q*-axis in the rotating reference frame system related to the PMSM rotor.

Other usual notations in the equations (1)-(4) are as following: the PMSM speed noted with ω; the flux linkage noted with λ_0; the PMSM number of pole pairs noted with n_p; the viscous friction coefficient noted with *B*; the PMSM rotor moment of inertia noted with *J*; the load torque of PMSM noted with T_L. To simplify, let us assume that: $L_d = L_q$ and $R_d = R_q = R_s$ [11-14].

Figure 1 shows the proposed architecture of the sensorless PMSM type control using the DTC control structure.

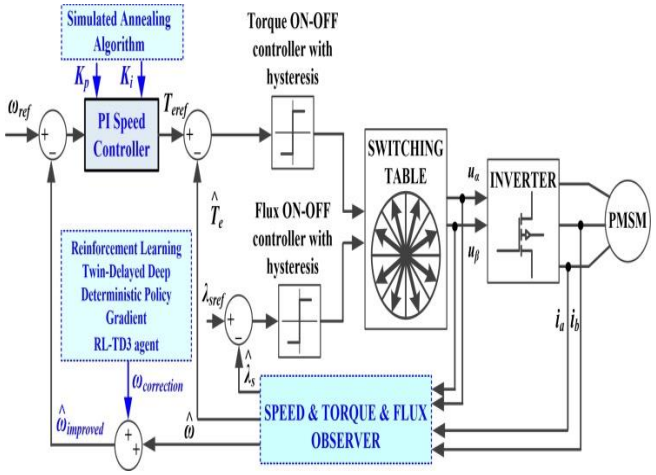

Fig. 1. Bloc diagram of the proposed PMSM sensorless control system based on DTC-type strategy.

For estimating the rotor speed, a speed observer using flux estimation is presented. In order to obtain improved performance, the speed observer will operate in combination with an RL-RD3 agent, and after proper training, the RL-RD3 agent will supply correction signals to help achieve a speed estimate closer to the measured speed for the PMSM control structure in the sensored case.

For the SMO-based description of observers, the description in *α-β* stationary reference frame related to the stator is usually used. In the case of DTC-type strategy, two cascaded control loops are used, an outer one based on a PI-type controller that performs the control for the PMSM rotor speed, while the inner control loops are very fast due to the use of ON-OFF hysteresis controllers, their role is to control the torque or currents and the flux. The connection equations used in the DTC-type control strategy in the *α-β* stationary reference frame are given in equations (5) and (6) [15].

$$\begin{cases} \lambda_\alpha = \int_0^t (u_\alpha - R_s i_\alpha) dt \\ \lambda_\beta = \int_0^t (u_\beta - R_s i_\beta) dt \end{cases} \quad (5)$$

$$\begin{cases} \bar{\lambda}_s = \sqrt{\hat{\lambda}_\alpha^2 + \hat{\lambda}_\beta^2} \\ \angle \hat{\lambda}_s = arctg \dfrac{\hat{\lambda}_\beta}{\hat{\lambda}_\alpha} \end{cases} \quad (6)$$

III. Improvement of the SMO Speed Observer Performances

To estimate the PMSM rotor speed according to [4], [6], an observer using an SMO technique is used to estimate the stator flux in the *α-β* stationary reference frame. The equations describing this observer are then completed to obtain the estimated PMSM rotor speed.

The use of an RL-TD3 type agent will result in an improved PMSM rotor speed estimate that will be closer to the measured speed.

A. Rotor Speed Observer Based on SMO

The equations for estimating the stator flux in the *α-β* reference frame are given in the next form (7) [4], [6].

$$\begin{cases} \dot{\hat{\lambda}}_\alpha = -R_s i_\alpha + u_\alpha + k_{1obs} \tilde{i}_\alpha + K_{1obs\_SMO} sigmoid(\tilde{i}_\alpha) \\ \dot{\hat{\lambda}}_\beta = -R_s i_\beta + u_\beta + k_{2obs} \tilde{i}_\beta + K_{2obs\_SMO} sigmoid(\tilde{i}_\beta) \end{cases} \quad (7)$$

where, usually the estimated variables are denoted by $\hat{\lambda}_\alpha$ and $\hat{\lambda}_\beta$, and the errors of the and currents $\tilde{i}_\alpha$ and $\tilde{i}_\beta$ in *α-β* frame are given by relation (8), while the estimation of the currents $\hat{i}_\alpha$ and $\hat{i}_\beta$ is expressed by relation (9).

$$\begin{cases} \tilde{i}_\alpha = i_\alpha - \hat{i}_\alpha \\ \tilde{i}_\beta = i_\beta - \hat{i}_\beta \end{cases} \quad (8)$$

$$\begin{cases} \hat{i}_\alpha = \dfrac{1}{L_d} \hat{\lambda}_\alpha + \dfrac{\lambda_0}{L_d} \cos(\hat{\theta}) \\ \hat{i}_\beta = \dfrac{1}{L_q} \hat{\lambda}_\beta - \dfrac{\lambda_0}{L_q} \sin(\hat{\theta}) \end{cases} \quad (9)$$

In the flux observer description equations (7), k_{1obs}, k_{2obs} K_{1obs_SMO}, and K_{2obs_SMO} are designed factors – gains of the observer.

Compared to the usual description of SMO in relation (7) we replaced the "*sign*" function by the "*sigmoid*" function [15], which has the role of achieving a smoothed transition between +1 and -1 and is given by relation (10) and plotted in Figure 2.

$$H(x) = \frac{2}{1 + e^{-a(x-c)}} - 1 \quad (10)$$

where: a is equal with 4 and c is equal with 0 are positive constants.

To estimate the mechanical PMSM rotor position, the next equation can be used (11).

$$\hat{\theta} = \tan^{-1}\left(\frac{\hat{\lambda}_{a\alpha}}{\hat{\lambda}_{a\beta}}\right) \tag{11}$$

with the next notations:

$$\begin{cases} \hat{\lambda}_{a\alpha} = \hat{\lambda}_{\alpha} - L_q i_{\alpha} \\ \hat{\lambda}_{a\beta} = \hat{\lambda}_{\beta} - L_q i_{\beta} \end{cases} \tag{12}$$

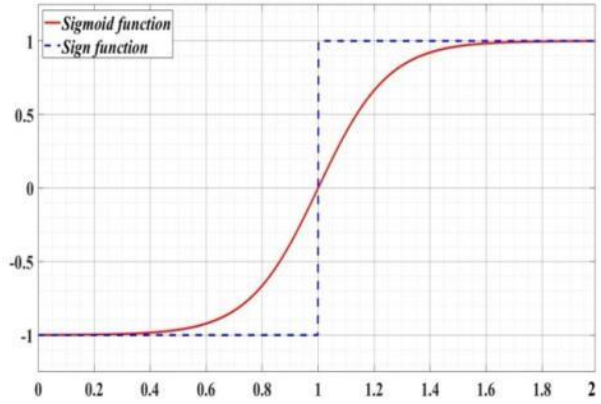

Fig. 2. Graphical representation of the sigmoid function $H(x)$.

The convergence of the observer is proved according to [4], [6], the Lyapunov function is defined as follows:

$$V = \frac{1}{2}\left(\tilde{\lambda}^T T^{-1} L^{-1} T \tilde{\lambda}\right) > 0 \tag{13}$$

where the transformation matrix $T\left(\hat{\theta}\right) = \begin{pmatrix} \cos\hat{\theta} & -\sin\hat{\theta} \\ \sin\hat{\theta} & \cos\hat{\theta} \end{pmatrix}$.

To estimate the electromagnetic torque, the following relation is used:

$$\hat{T}_e = \frac{3}{2} n_p \left(\hat{\lambda}_{\alpha} i_{\alpha} - \hat{\lambda}_{\beta} i_{\beta}\right) \tag{14}$$

Based on this, the PMSM rotor speed estimation is given by the following relation:

$$\hat{\omega} = \frac{\hat{\lambda}_{a\alpha(k-1)}\hat{\lambda}_{a\beta(k)} - \hat{\lambda}_{a\beta(k-1)}\hat{\lambda}_{a\alpha(k)}}{T_s\left(\hat{\lambda}^2_{a\alpha(k)} + \hat{\lambda}^2_{a\beta(k)}\right)} \tag{15}$$

where Ts represents the sampling period, the current sampling step is denoted by k.

B. Simulated Annealing Algorithm

Starting from the PID speed controller equation, this section presents a computational intelligence algorithm for optimizing the controller tuning parameters. In relation (16), the equation describing a PID controller is presented, with the mention that in the present application K_d = 0 is customized, obtaining in practice a PI controller. The PI controller output noted $u(t)$ in relation (16), integrated in the cascade control structure presented in Section II, will represent the reference size of the torque control loop.

$$u(t) = K_p e(t) + K_i \int_0^t e(t)dt + K_d \frac{de(t)}{dt} \tag{16}$$

The SA algorithm can be seen as an analogy of the cooling process of a solid. At low temperatures the mobility of the molecules decreases and an alignment of the structure corresponding to a minimum energy state of the system is achieved. This minimum energy of the system can be equated with reaching a minimum of an objective function. Calculate the probability of selection of the next state based on the Boltzmann-Gibbs distribution where T is the temperature parameter [19, 20].

$$\varphi\left(x_i(t)\right) = \frac{1}{1 + e^{f\left(\frac{x_i(t)}{T(t)}\right)}} \tag{17}$$

The probability of movement from point x_i to point x_j can be expressed by the following expression:

$$P_{ij} = \begin{cases} 1; & if\ f\left(x_j\right) < f\left(x_i\right) \\ e^{-\frac{f\left(x_j\right) - f\left(x_i\right)}{c_b T}}; & altfel \end{cases} \tag{18}$$

where: c_b represents the Boltzman constant.

At each step of the algorithm a new solution is generated as:

$$x(t+1) = x(t) + D(t)r(t) \tag{19}$$

where: $r(t) \approx U(-1,1)^{n_x}$ and D is a matrix of the maximum allowable change for each variable.

The evolution of the state is completed by the following expression:

$$D(t+1) = (1-\alpha)D(t) + \alpha\omega R(t) \tag{20}$$

where: $R(t)$ represents a diagonal matrix whose elements are the magnitudes of the successful changes, and α and ω are constants.

The following relations is used to decrease the temperature:

$$T(t+1) = \alpha T(t); \quad \alpha \in (0,1) \tag{21}$$

C. RL-TD3 Agent for Improvement of the PMSM Rotor Speed Estimation

The deployment of the RL-TD3 agent in this case consists of creating, training, and deploying it to work in tandem with the speed observer presented above. The RL-TD3 agent's operation is based on minimizing a reward, such as that in relation (22) [21].

$$r_{RL\_SMO} = -\left(5\omega_{error}^2 + 0.1\sum_j \left(u_{t-1}^j\right)^2\right) \quad (22)$$

where the last term u_{t-1}^j represents the action value in the previous iteration.

After the training process, the RL-TD3 agent will supply correction signals to the PMSM speed observer to obtain an estimate as close to the PMSM rotor speed measured value as possible.

IV. MATLAB/SIMULINK IMPLEMENTATION AND NUMERICAL SIMULATIONS

The numerical simulations presented in this section are achieved in the Matlab/Simulink programming environment.

Figure 3 presents the Matlab/Simulink model implementation block diagram for the PMSM sensorless control system based on a DTC-type strategy and a SMO observer employing a RL-TD3 agent for PMSM rotor speed estimation. Matlab/Simulink implementation of the rotor speed observer is presented in Figure 4.

The Matlab/Simulink implementation is achieved based on equations (7)-(15).

The designed factors of the SMO-type observer are set to the next values: k_{1obs} = 150, k_2 = 50, K_{1obs_SMO} = 0.1, and K_{2obs_SMO} = 0.1.

The nominal PMSM parameters used in these numerical simulations performed in Matlab/Simulink programming environment are shown in Table I.

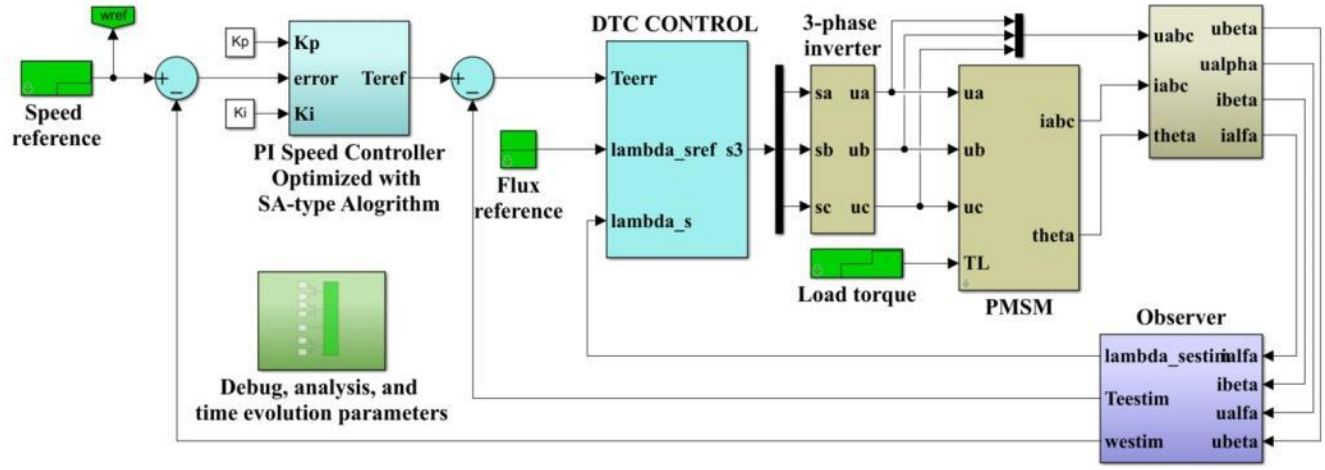

Fig. 3. Matlab/Simulink model implementation of the based on DTC strategy using PI speed controller optimized with SA-type algorithm and SMO-type observer employing a RL-TD3 agent for speed estimation.

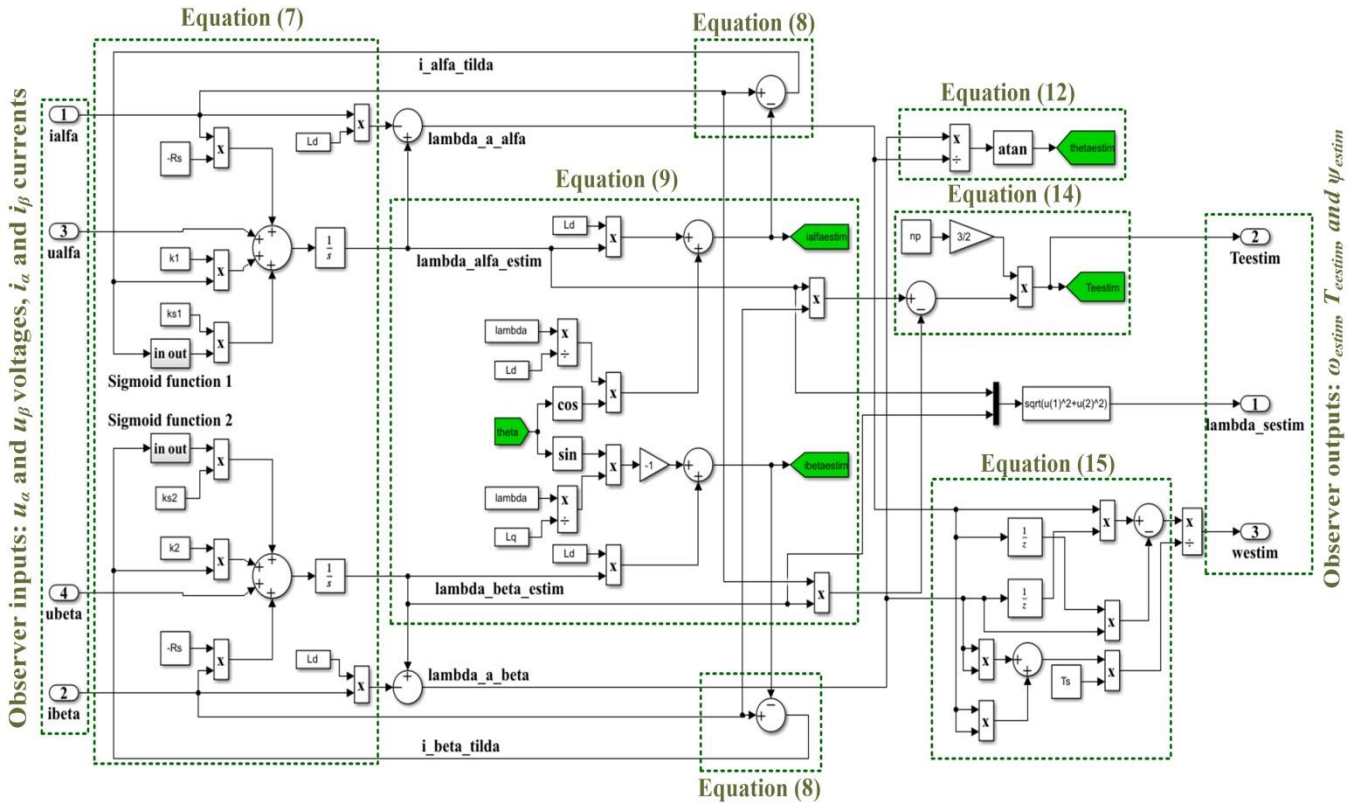

Fig. 4. Matlab/Simulink subsystem implementation of the SMO observer.

TABLE I. THE NOMINAL VALUES OF PMSM PARAMETERS.

Parameter	Value	Unit
R_s – PMSM stator resistance	2.875	Ω
L_q and L_d – PMSM inductances on *d-q* rotating reference frame	0.0085	H
J – combined inertia of rotor and load	0.0008	kg·m^2
B – combined viscous friction of rotor and load	0.005	N·m·s/rad
λ_0 – flux induced by the permanent magnets of the rotor in the stator phases	0.175	Wb
n_P – PMSM pole pairs number	4	-

The block diagram for the Matlab/Simulink subsystem implementation of RL-TD3 agent algorithm is shown in Figure 5, and the reward is given by relation (22) and the observations of the RL-TD3 agent are rotor speed and rotor speed error. Also, Figure 6 show the performance of the reward while the training stage of RL-TD3 algorithm is running for 200 episode number.

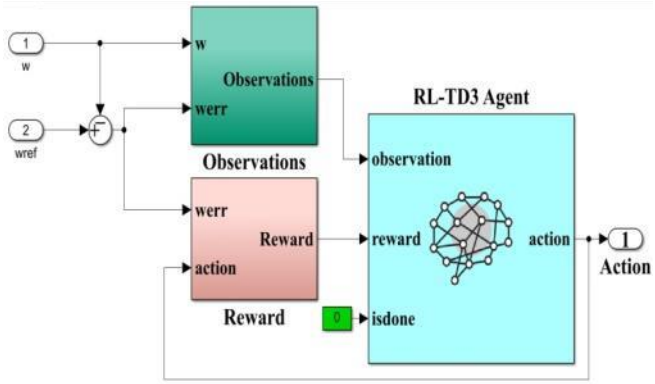

Fig. 5. Block diagram of the Matlab/Simulink subsystem implementation for RL-TD3 agent algorithm.

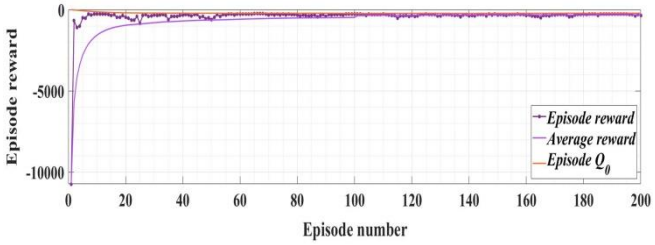

Fig. 6. Performance of the reward during training stage of the RL-TD3 agent algorithm.

Figure 7 presents the flux space vector trajectory in α-β stationary reference frame coordinates for the case of the PMSM control system based DTC strategy.

Regarding the stator flux and torque estimates based on equations (7) and (14), Figures 8 and 9 respectively show the results of the numerical simulations. These simulations were performed for a PMSM for the nominal parameters given in Table I, and the speed controller was tuned using an SA-type algorithm. Good flux and torque estimation results are observed, estimates that will enter as reaction quantities in the flux and torque contour loops of the DTC control strategy. Note that in this case, following the traditional configuration of single-input ON-OFF controllers with hysteresis, all attention will be paid to the PMSM rotor speed estimation performance, rather than the torque and flux estimation performance.

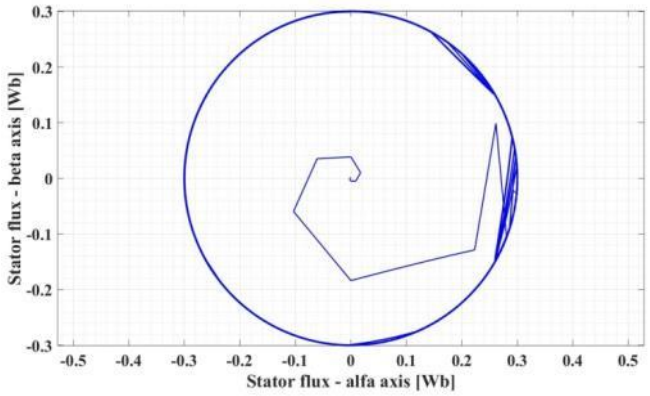

Fig. 7. Flux space vector trajectory in the case of the PMSM control system based DTC strategy.

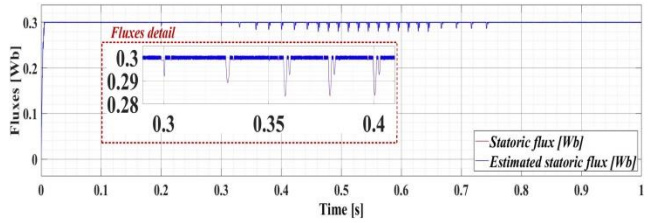

Fig. 8. Measured statoric flux versus estiamted statoric flux in case of the PMSM control system using DTC strategy.

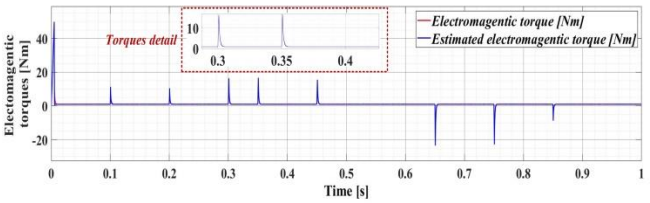

Fig. 9. Measured torque versus estiamted torque in case of the PMSM control system using DTC strategy.

Based on the nominal PMSM parameters presented in Table I for the case of the PMSM sensored control system based on DTC strategy using PI peed controller optimized using SA-type algorithm, Figure 10 presents the time evolution of the control system. This presents the time evolution of the next parameters: PMSM rotor speed, PMSM reference speed, load and electromagnetic torques, stator currents i_a, i_b, i_c, and fluxes on α-β stationary reference frame. The speed reference signal ω_{ref} used in the numerical simulations is expressed as a sequence of steps: [100 200 300 500 700 900 600 300 200]rpm→[0 0.1 0.2 0.3 0.35 0.45 0.65 0.75 0.85]s.

In the case of PMSM speed estimation using the presented observer in Section III, Figure 10 presents the time evolution of the PMSM sensorless control system based on DTC strategy using PI speed controller optimized using SA-type algorithm and the SMO-type observer. Also, Figures 11 and 12 presents the time evolution of the PMSM sensorless control system based on DTC strategy using PI speed controller optimized using SA-type algorithm and the SMO-type observer in tandem with the RL-TD3 agent for improvement of speed estimation.

A comparison between the PMSM rotor speed in the sensored and sensorless case based on a speed observer and a speed observer combined with an RL-TD3 agent is presented in Figure 13.

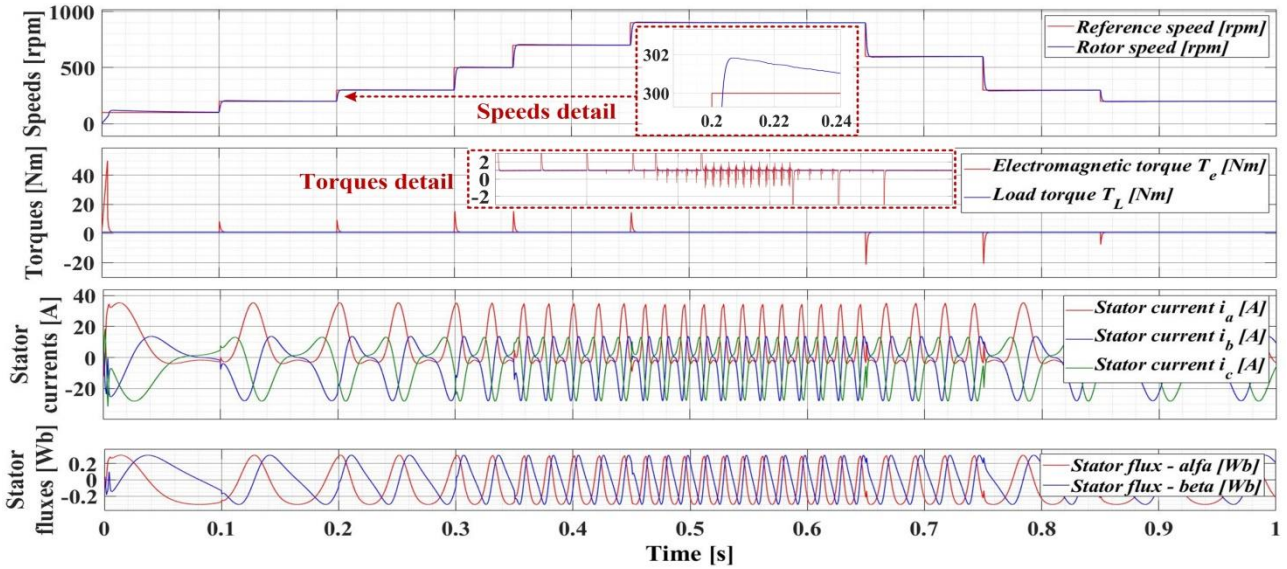

Fig. 10. Time evolution of the PMSM sensored control system based on DTC strategy using PI speed controller optimized with SA-type algorithm.

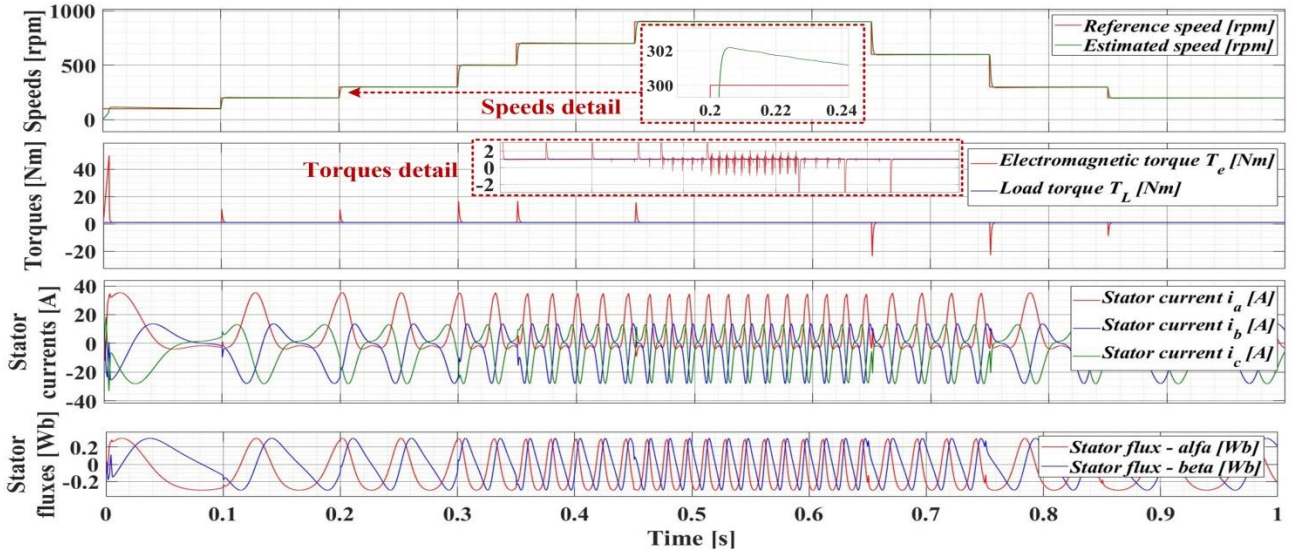

Fig. 11. Time evolution of the PMSM sensorless control system based on DTC strategy using PI speed controller optimized with SA-type algorithm and SMO-type observer.

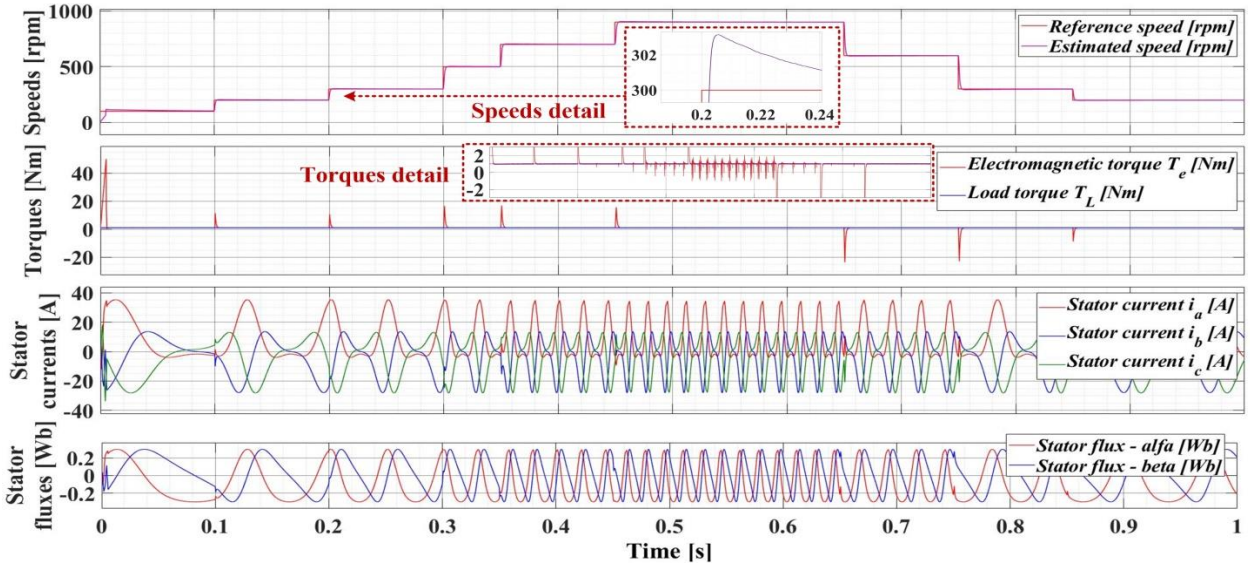

Fig. 12. Time evolution of the PMSM sensorless control system based on DTC strategy using PI speed controller optimized with SA-type algorithm and SMO-type observer combined with RL-TD3 agent.

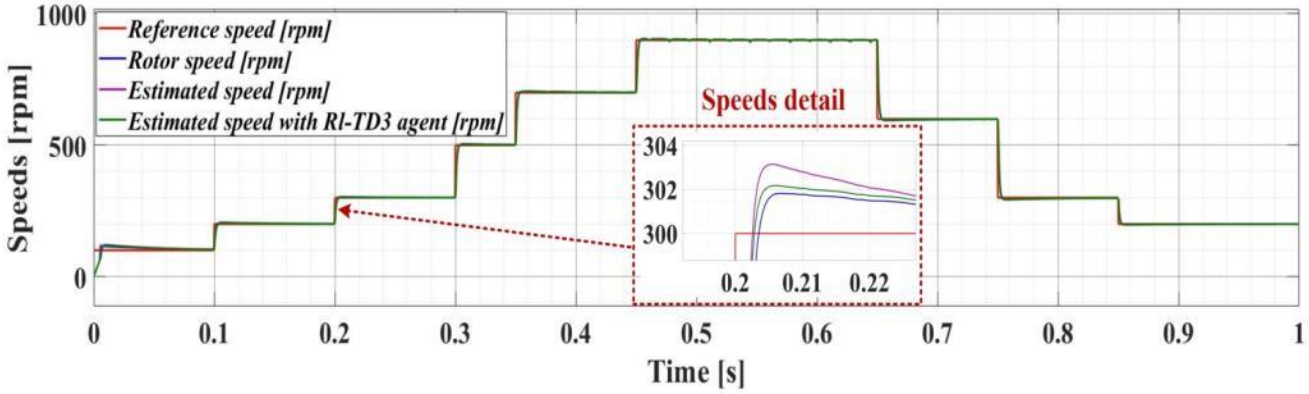

Fig. 13. Time evolution comparison for the measured speed and estimated speed (SMO speed observer and SMO speed observer in tandem with RL-TD3-type agent).

Table II summarizes the achievement of the PMSM rotor speed observer performances (with and without RL-TD3 agent) compared with the case of the sensored control structure. The criteria for comparison are based on the next quality indicators: response time, PMSM rotor speed ripple and overshoot. It can be noted that the employing of the RL-TD3-type agent in combination with the basic SMO-type speed observer leads to an improvement in its performance, providing a speed estimate close to the measured PMSM rotor speed.

The PMSM speed ripple is defined in the following expression:

$$\omega_{ripple} = \sqrt{\frac{1}{N}\sum_{i=1}^{N}\left(\omega(i) - \omega_{ref}(i)\right)^2} \qquad (23)$$

where: N represents the number of samples, ω represents the PMSM speed; ω_{ref} represents the PMSM reference speed.

TABLE II. PERFORMANCES OF THE PMSM SENSORLESS CONTROL SYSTEM USING IMPROVED SMO-TYPE OBSERVER.

PMSM rotor speed	Response time [ms]	Rotor speed ripple [rpm]	Overshooting [%]
Measured	3.5	16.109	0.6
Estimated with SMO observer	2.8	16.623	0.9
Estimated with SMO observer combined with RL-TD3 agent	2.6	16.291	0.7

V. CONCLUSIONS

This paper presents a way to improve the PMSM rotor speed estimation when using the DTC control strategy by employing an RL-TD3-type agent together with an SMO speed observer. The tuning parameters of the PI speed controller are obtained using an SA-type algorithm. The article presents the control structures and PMSM operating equations, the DTC-type control strategy and the SMO observer. The implementations of these control structures and algorithms were performed in the Matlab/Simulink programming environment and showed through numerical simulations the improvements to the SMO speed observer by using an RL-TD3-type agent. Future work will analyze other ways to improve PMSM rotor speed estimation in the case of DTC control strategy. Also, will be analyzed a controller that, in addition to the main task presented above, will facilitate obtaining currents as close to the sinusoidal form as possible and a Total Harmonic Distortion (THD) as low as possible.

REFERENCES

[1] T. H. Nguyen, T. T. Nguyen, K. Minh Le, H. N. Tran, J. W. Jeon, "An Adaptive Backstepping Sliding-Mode Control for Improving Position Tracking of a Permanent-Magnet Synchronous Motor With a Nonlinear Disturbance Observer," in IEEE Access, vol. 11, pp. 19173-19185, February 2023.

[2] X. Lin *et al.*, "Observer-Based Fixed-Time Control for Permanent-Magnet Synchronous Motors With Parameter Uncertainties," in IEEE Transactions on Power Electronics, vol. 38, no. 4, pp. 4335-4344, April 2023.

[3] Y. Fan, J. Chen, Q. Zhang, M. Cheng, "An Improved Inertia Disturbance Suppression Method for PMSM Based on Disturbance Observer and Two-Degree-of-Freedom PI Controller," in IEEE Transactions on Power Electronics, vol. 38, no. 3, pp. 3590-3599, March 2023.

[4] G. H. B. Foo and M. F. Rahman, "Direct Torque Control of an IPM-Synchronous Motor Drive at Very Low Speed Using a Sliding-Mode Stator Flux Observer," in IEEE Transactions on Power Electronics, vol. 25, no. 4, pp. 933-942, April 2010.

[5] Y. Zheng, Z. Cao, Z. Man, A. Kumar, S. Wang, "Phase-lead Repetitive Control of a PMSM with Field-oriented Feedback Linearization and a disturbance observer," *IECON 2021 – 47th Annual Conference of the IEEE Industrial Electronics Society*, Toronto, ON, Canada, 2021, pp. 1-4.

[6] M. N. Nicola and C. -I. Nicola, "Improvement Performances of Sensorless Control for PMSM Based on DTC Strategy Using SMO Observer and RL-TD3 Agent," *5th Global Power, Energy and Communication Conference (GPECOM)*, Nevsehir, Turkiye, 2023, pp. 131-136.

[7] X. Zhang, X. Xie, R. Yao, "Field oriented control for permanent magnet synchronous motor based on DSP experimental platform," *The 27th Chinese Control and Decision Conference (2015 CCDC)*, Qingdao, China, 2015, pp. 1870-1875.

[8] C. -I. Nicola and M. Nicola, "Real Time Implementation of the PMSM Sensorless Control Based on FOC Strategy," *4th Global Power, Energy and Communication Conference (GPECOM)*, Nevsehir, Turkey, 2022, pp. 179-183.

[9] L. Qi, Z. Yong, Z. Chao, W. Man, "Research on rotor field-oriented vector control of PMSM for aircraft electro-mechanical actuator," *Chinese Control and Decision Conference (CCDC)*, Yinchuan, China, 2016, pp. 6422-6427.

[10] R. G. Iturra and P. Thiemann, "Sensorless Field Oriented Control of PMSM using Direct Flux Control with improved measurement sequence," *XVIII International Scientific Technical Conference Alternating Current Electric Drives (ACED)*, Ekaterinburg, Russia, 2021, pp. 1-6.

[11] K. V. P. Kumar and T. V. Kumar, "Improvised direct torque control strategies of open end winding PMSM fed with multi-level

inversion," *IEEE International Conference on Industrial Technology (ICIT)*, Lyon, France, 2018, pp. 425-430.

[12] M. Nicola, C. -I. Nicola, D. Sacerdoţianu, "Sensorless Control of PMSM using DTC Strategy Based on PI-ILC Law and MRAS Observer," *International Conference on Development and Application Systems (DAS)*, Suceava, Romania, 2020, pp. 38-43.

[13] W. Wu, F. Xie, G. Li, K. Liang, C. Qiu, H. Jiang, "Research on Direct Torque Control Based on RZVSVPWM of PMSM," *14th IEEE Conference on Industrial Electronics and Applications (ICIEA)*, Xi'an, China, 2019, pp. 2507-2511.

[14] A. Vujji and R. Dahiya, "Design of PI Controller for Space Vector Modulation based Direct Flux and Torque Control of PMSM Drive," *First IEEE International Conference on Measurement, Instrumentation, Control and Automation (ICMICA)*, Kurukshetra, India, 2020, pp. 1-6.

[15] M. Nicola and C. -I. Nicola, "Sensorless Control for PMSM Using Model Reference Adaptive Control and back-EMF Sliding Mode Observer," *International Conference on Electromechanical and Energy Systems (SIELMEN)*, Craiova, Romania, 2019, pp. 1-7.

[16] I. Tangirala, T. Ramesh, P. D. Kumar, R. Pothuraju, "Sensorless control of Five level inverter fed Fuzzy Logic based DTFC SVM Controlled PMSM drive using Luenberger Observer," *IEEE IAS Global Conference on Emerging Technologies (GlobConET)*, Arad, Romania, 2022, pp. 852-857.

[17] S. S. Badini and V. Verma, "A Novel MRAS Based Speed Sensorless Vector Controlled PMSM Drive," *54th International Universities Power Engineering Conference (UPEC)*, Bucharest, Romania, 2019, pp. 1-6.

[18] H. Li and Z. Wang, "Sensorless Control for PMSM Drives Using the Cubature Kalman Filter based Speed and Flux Observer," *IEEE International Conference on Electrical Systems for Aircraft, Railway, Ship Propulsion and Road Vehicles & International Transportation Electrification Conference (ESARS-ITEC)*, Nottingham, UK, 2018, pp. 1-6.

[19] G. Yi, W. Zhou, S. Li, Y. Chen, "Access Craft Scheduling of Stereo Garage Based on Improved Hybrid Simulated Annealing Algorithm," *4th International Conference on Robotics, Control and Automation Engineering (RCAE)*, Wuhan, China, 2021, pp. 423-427.

[20] B. Aylaj and S. Nouh, "Degeneration vs Classical of simulated annealing algorithm: performance analysis," *5th International Conference on Advanced Communication Technologies and Networking (CommNet)*, Marrakech, Morocco, 2022, pp. 1-5.

[21] M. Nicola and C. -I. Nicola, "Improvement of PMSM Control Using Reinforcement Learning Deep Deterministic Policy Gradient Agent," *21st International Symposium on Power Electronics (Ee)*, Novi Sad, Serbia, 2021, pp. 1-6.

[22] Reinforcement Learning Toolbox™ User's Guide, Matlab and Simulink, MathWorks, Natick, MA, USA, 2020.

[23] P. Brandimarte, From Shortest Paths to Reinforcement Learning: A MATLAB-Based Tutorial on Dynamic Programming, Springer Nature, 2021.

[24] R. S. Sutton and A. G. Barto, Reinforcement Learning An Introduction, second edition, The MIT Press, London, England, 2018..